Electronic Supplementary Information for:

Synthesis and characterization of low-nuclearity lantern-type porous coordination cages

Garrett A. Taggart,[a] Gregory R. Lorzing,[a,b] Michael R. Dworzak,[a] Glenn P. A. Yap,[a] and Eric D. Bloch*[a,b]

[a]Department of Chemistry and Biochemistry, University of Delaware, Newark, Delaware 19716, United States

[b]Center for Neutron Science, Department of Chemical and Biomolecular Engineering, University of Delaware, Newark, Delaware 19716, USA

Table of Contents

General Considerations

^{1}H-NMR spectra were taken on a Bruker 400 MHz spectrometer with a 5-mm Bruker SMART probe and data obtained was manipulated in MestReNova NMR processor software. Infrared (IR) Spectroscopy measurements were carried out with a Bruker ALPHA II. IR spectra of activated cage samples were recorded by suspending cage in degassed paratone oil.

Synthesis of $Cr_2(OAc)_4$.[1] The material was synthesized via a modified literature procedure. In a dry, 250 mL round-bottom flask, add Cr powder (2.9699 g, 57.11 mmol) and HBr (2 mL) to a solution of acetic acid (80 mL) and acetic anhydride (20 mL). The solution was refluxed under nitrogen for 48 hours. Upon cooling, a brick red powder precipitates. The powder was quickly filtered using a swivel frit and washed with diethyl ether under N_2. The solid was quickly transferred into an N_2-atmosphere glovebox.

Ligand Syntheses:

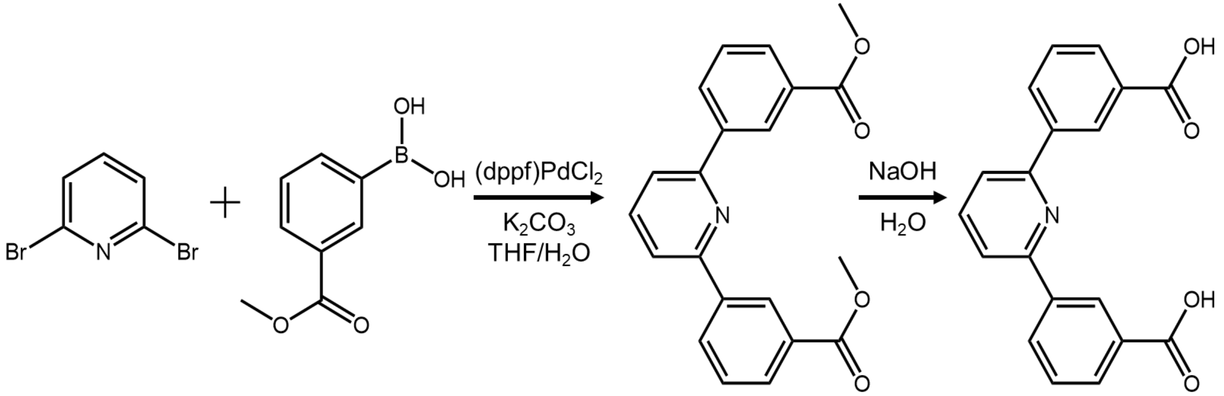

Synthesis of pyridinedibenzoate (H_2pdb)[2]: 2,6-dibromopyridine (3.9015 g, 16.4697 mmol) and 3-methoxycarbonylphenylboronic acid (7.2221 g, 40.1295 mmol) were added to a 3-neck round bottom flask and dissolved in 300 mL of THF. Potassium carbonate (9.971 g) was dissolved in 50 mL of water and the carbonate solution was then added to the flask. A water condenser with a N_2 line connected was attached and rubber stoppers were placed on the other necks. The atmosphere was purged with N_2 for 1 hour before [1,1'-Bis(diphenylphosphino)ferrocene]palladium(II) dichloride (0.4047 g, 0.5531 mmol) was quickly added while under positive N_2 pressure. The flask was sealed and heated to 80 °C overnight. Volatile solvent was removed via rotary evaporation, then water and sodium hydroxide was added and the flask was heated to 100 °C without isolating the product. The solution was filtered through a celite plug and the filtrate was acidified very slowly with HCl. The precipitate was then filtered out via vacuum filtration and dried yielding (97.43 %) high purity product. ^{1}H NMR (400 MHz, DMSO-d_6): $\delta = 8.74$ (t, 2H, arom), 8.45 (d of t, 2H, arom), 8.06 (t, 1H, arom), 8.04 (s, 4H, arom), 7.69 (t, 2H, arom).

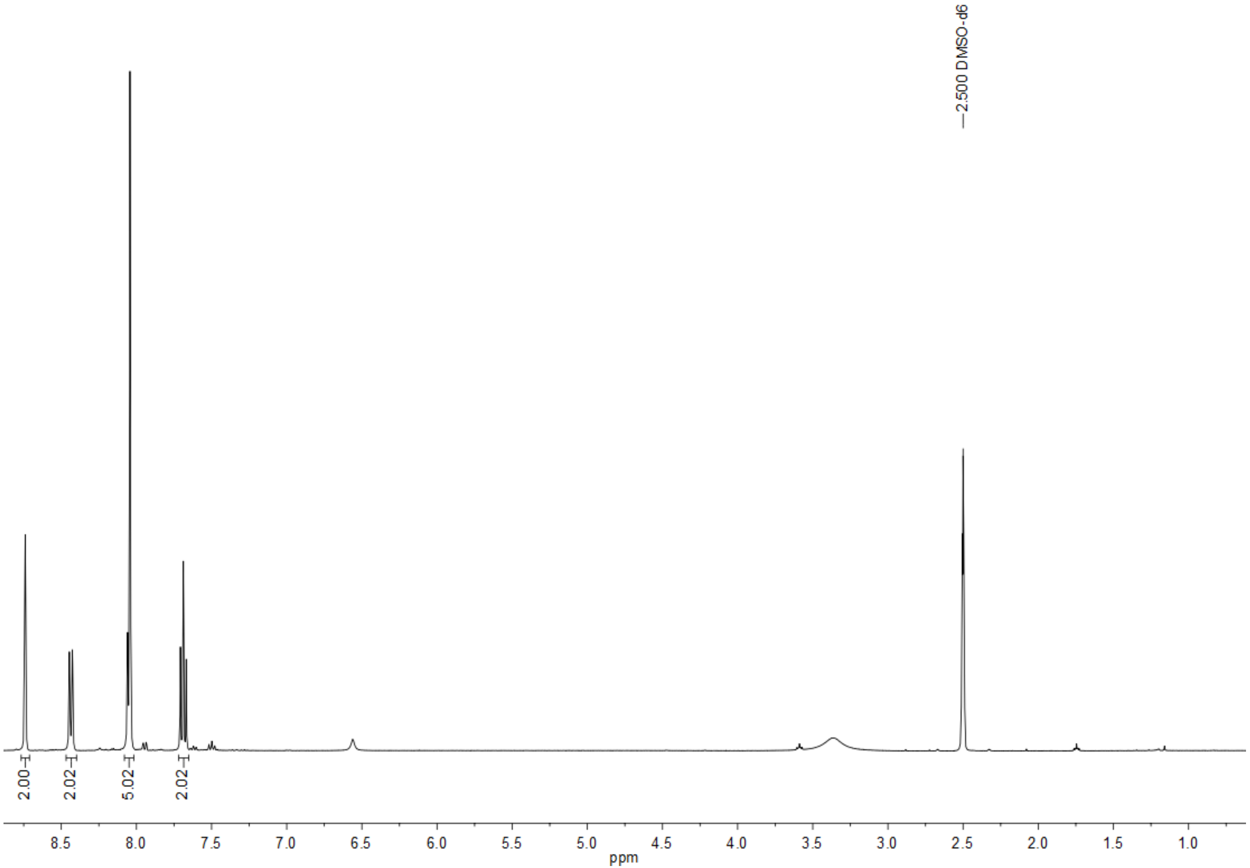

Figure S1. ^{1}H NMR spectrum of (H_2pdb) ligand in DMSO-d_6.

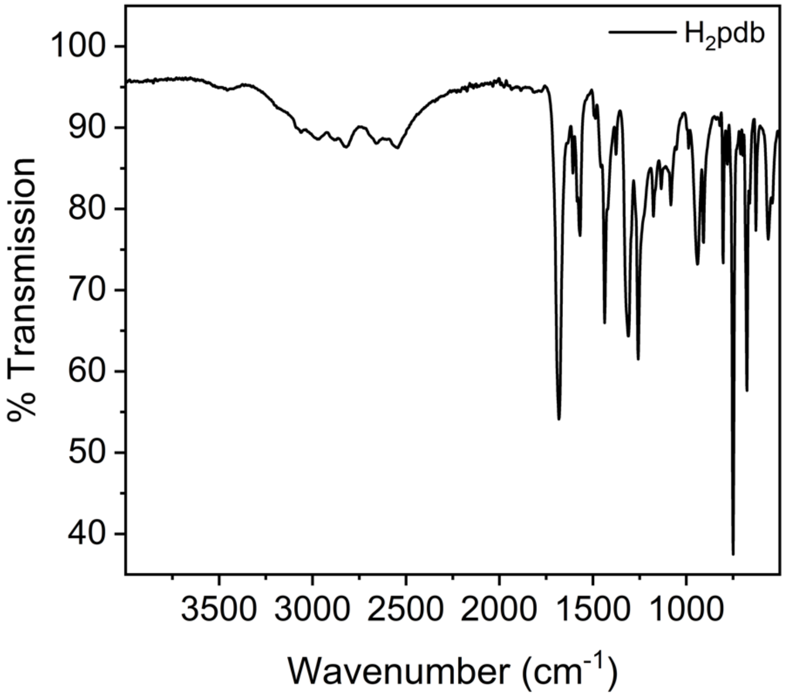

Figure S2. IR spectrum of (H_2pdb) ligand.

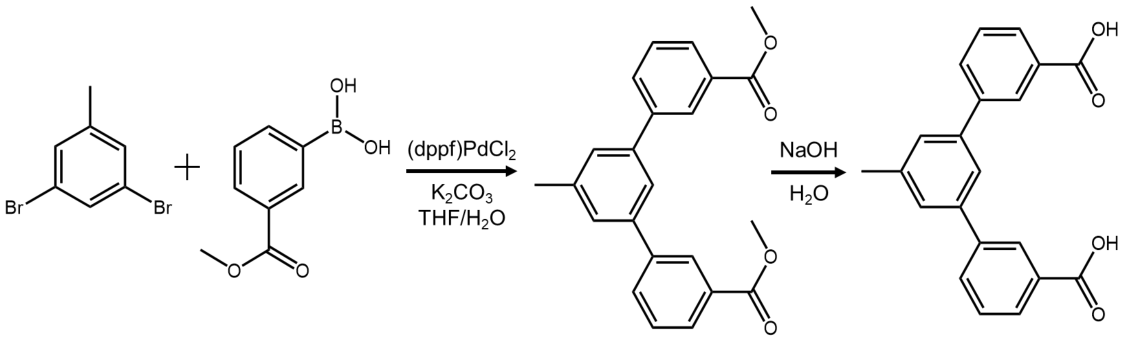

Synthesis of toluenedibenzoate (H_2tdb)[3]: 3,5-dibromotoluene (5.5264 g, 22.1118 mmol) and 3-methoxycarbonylphenylboronic acid (8.4524 g, 46.9656 mmol) were added to a 3-neck round bottom flask and dissolved in 300 mL of THF. Potassium carbonate (12.903 g) was dissolved in 50 mL of water and the carbonate solution was then added to the flask. A water condenser with a N_2 line connected was attached and rubber stoppers were placed on the other necks. The atmosphere was purged with N_2 for 1 hour before [1,1'-Bis(diphenylphosphino)ferrocene]palladium(II) dichloride (0.5051 g, 0.6903 mmol) was quickly added while under positive N_2 pressure. The flask was sealed and heated to 80 °C overnight. Volatile solvent was removed via rotary evaporation, then water and sodium hydroxide was added and the flask was heated to 100 °C without isolating the product. The solution was filtered through a celite plug and the filtrate was acidified very slowly with HCl. The precipitate was then filtered out via vacuum filtration and dried yielding 6.6966 g (91.12 %) of high purity product. ^{1}H NMR (400 MHz, DMSO-d_6): δ = 8.26 (s, 2H, arom), 8.02 (d, 2H, arom), 7.97 (d, 2H, arom), 7.75 (s, 1H, arom), 7.62 (t, 2H, arom), 7.55 (s, 2H, arom), 2.47 (s, 3H, methyl).

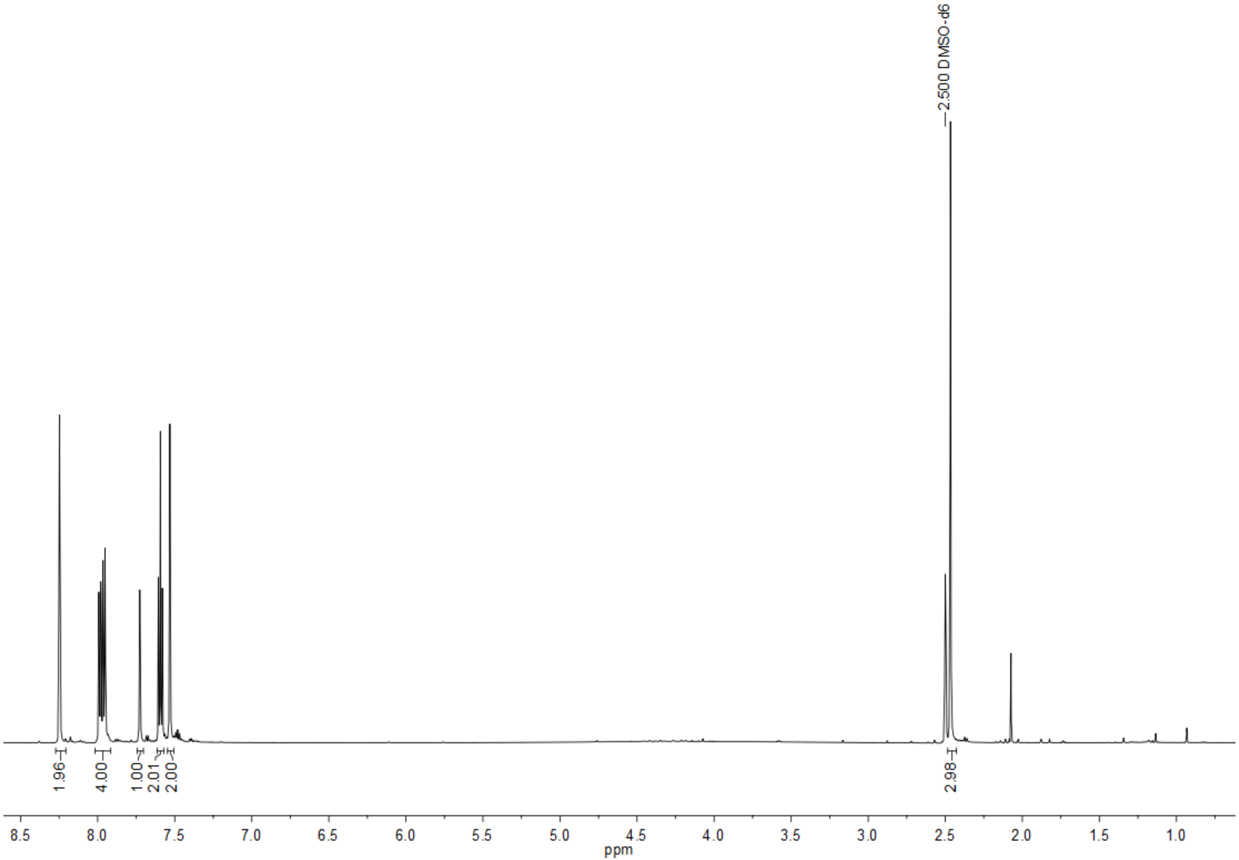

Figure S3. ^{1}H NMR spectrum of H_2tdb ligand in DMSO-d_6.

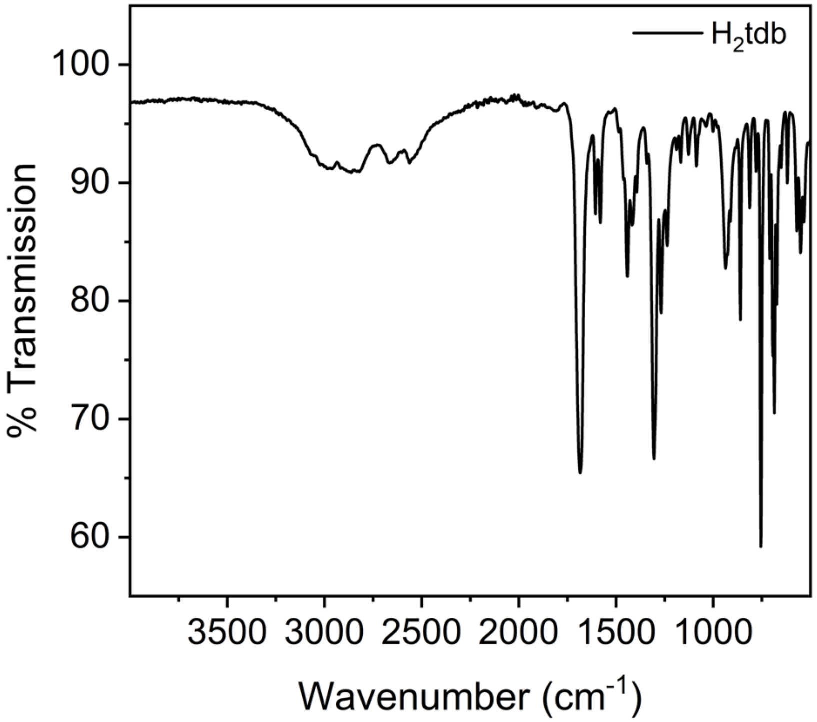

Figure S4. IR spectrum of H_2tdb ligand.

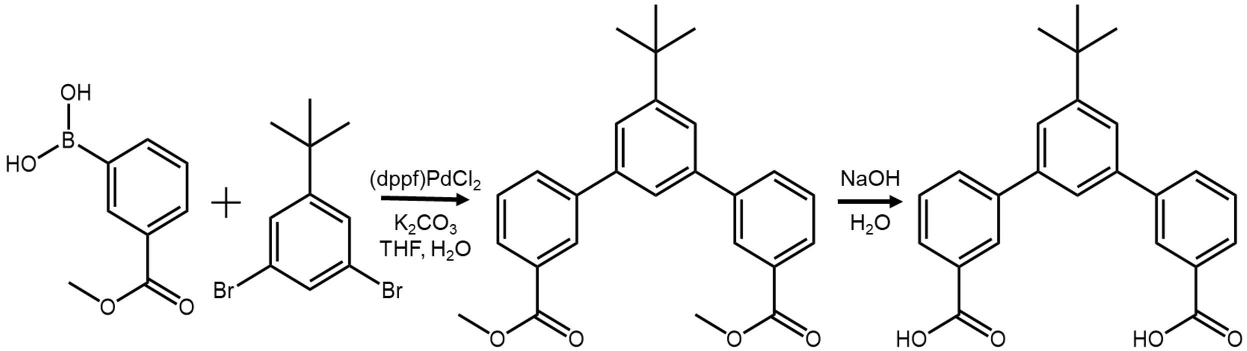

Synthesis of *tert*-butylbenzene-1,3-dibenzoate ($H_2{}^t$bu-bdb): 1,3-Dibromo-5-*tert*-butylbenzene (4 mL, 13.69mmol) and 3-methoxycarbonylphenylboronic acid (5.6820 g, 31.56mmol) were added to a 3-neck round bottom flask and dissolved in 300 mL of THF. Potassium carbonate (7.675g) was dissolved in 50 mL of water and the carbonate solution was then added to the flask. A water condenser with a N_2 line connected was attached and rubber stoppers were placed on the other necks. The atmosphere was purged with N_2 for 1 hour before [1,1'-Bis(diphenylphosphino)ferrocene]palladium(II) dichloride (0.2586 g, 0.3534 mmol) was quickly added while under positive N_2 pressure. The flask was sealed and heated to 80 °C overnight. Volatile solvent was removed via rotary evaporation, then water and sodium hydroxide was added and the flask was heated to 100 °C without isolating the product. The solution was filtered through a celite plug and the filtrate was acidified very slowly with HCl. The precipitate was then filtered out via vacuum filtration and dried yielding 8.7891 g (58.48 %) of high purity product. ^{1}H NMR (400 MHz, DMSO-d_6): δ = 8.24 (s, 2H, arom), 8.02 (d, 2H, arom), 7.96 (d, 2H, arom), 7.73 (t, 1H, arom), 7.69 (s, 2H, arom), 7.62 (t, 2H, arom), 1.41 (s, 9H, *tert*-butyl).

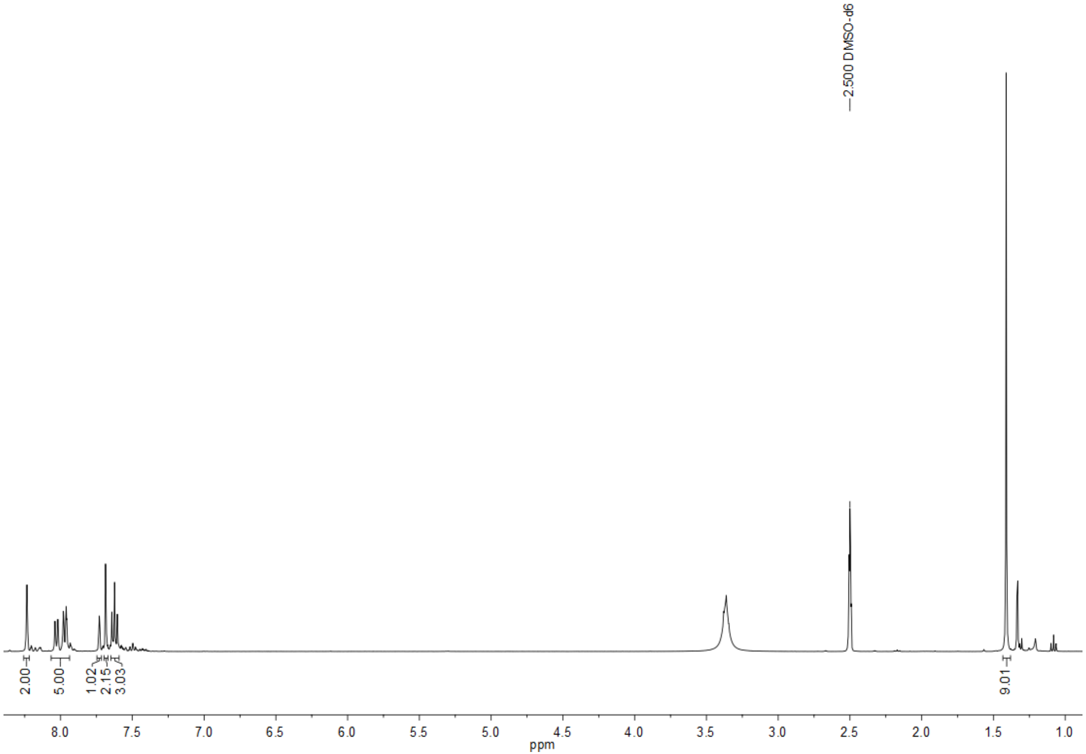

Figure S5. ^{1}H NMR spectrum of $H_2{}^t$bu-bdb ligand in DMSO-d$_6$.

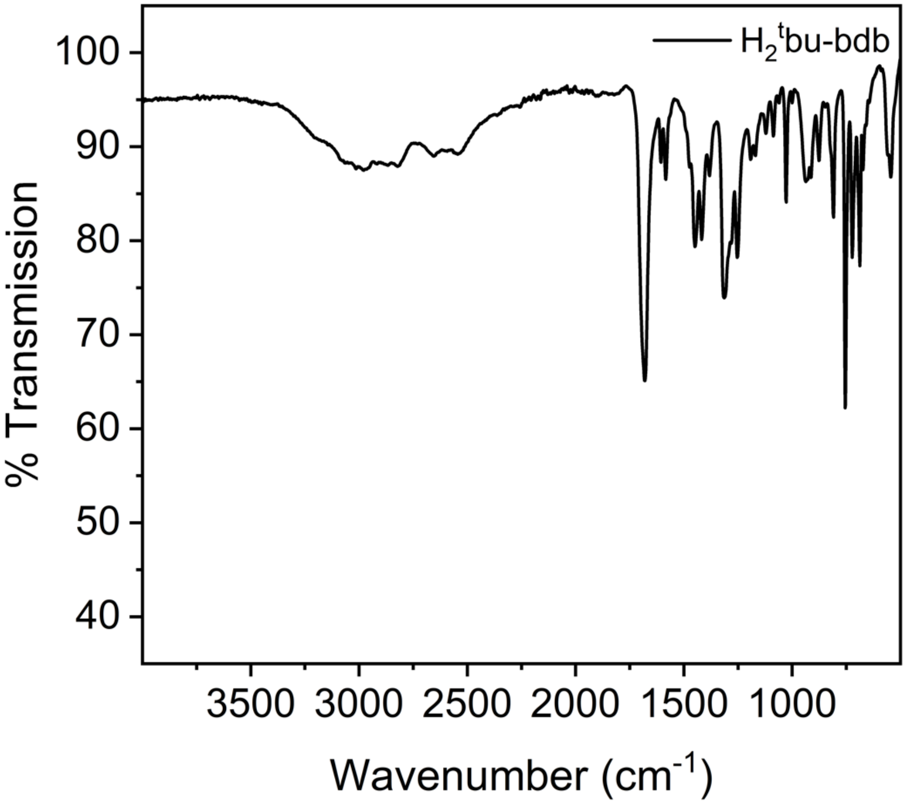

Figure S6. IR spectrum of $H_2{}^t$bu-bdb.

Cage Synthesis:

Synthesis of $Cu_4(pdb)_4$: Copper(II) nitrate hemipentahydrate (0.1678 g, 0.7214 mmol) and H_2pdb (0.2065 g, 0.6467 mmol) were added to a 20 mL scintillation vial. The contents were dissolved in 17 mL of DMF and 3 mL of methanol were carefully layered on top of the solution. The vial was placed in an aluminum block and heated to 80 °C overnight, yielding single crystal quality product. Solvent was decanted off and the sample was washed with methanol three times before being activated *in vacuo* for gas adsorption measurements.

Synthesis of $Cu_4(^tbu\text{-}bdb)_4$: Copper(II) nitrate hemipentahydrate (0.1676 g, 0.7205 mmol) and $H_2{}^t$bu-bdb (0.2179 g, 0.5820 mmol) were added to a 20 mL scintillation vial. The contents were dissolved in 17 mL of DMF and 3 mL of methanol were carefully layered on top of the solution. The vial was placed in an aluminum block and heated to 80 °C overnight, yielding a green powder. Solvent was decanted off and the sample was washed with methanol three times before being activated *in vacuo* for gas adsorption measurements.

Synthesis of $Cu_4(tdb)_4$: Copper(II) nitrate hemipentahydrate (0.1539 g, 0.6617 mmol) and H_2tdb (0.2043 g, 0.6147 mmol) were added to a 20 mL scintillation vial. The contents were dissolved in 17 mL of DMF and 3 mL of methanol were carefully layered on top of the solution. The vial was placed in an aluminum block and heated to 80 °C overnight, yielding single crystal quality product. Solvent was decanted off and the sample was washed with methanol three times before being activated *in vacuo* for gas adsorption measurements.

Synthesis of $Cr_4(tdb)_4$: All syntheses were carried out under an N_2 atmosphere in a glove box and all solvents used were anhydrous. Chromium(II) acetate (0.1135 g, 0.6677mmol) and H_2tdb (0.3078 g, 0.9261 mmol) were added to a 20 mL scintillation vial. Ligand and salt were dissolved in 17 mL of DMF and the vials were heated to 80 °C for an hour to fully dissolve the salt. The solution was carefully decanted from the left-over precipitate and approximately 3 mL of methanol were added to the solutions. The vials were heated to 80 °C overnight yielding crystalline solid.

Synthesis of $Mo_4(tdb)_4$: All syntheses were carried out under an N_2 atmosphere in a glove box and all solvents used were anhydrous. Molybdenum(II) acetate (0.1203 g, 0.2336 mmol) and H_2tdb (0.3211 g, 0.9672 mmol) were added to a 20 mL scintillation vial. Ligand and salt were dissolved in 17 mL of DMF and the vials were heated to 80 °C for an hour to fully dissolve the salt. The solution was carefully decanted from the left-over precipitate and approximately 3 mL of methanol were added to the solutions. The vials were heated to 80 °C overnight yielding crystalline solid.

Cage IR spectra:

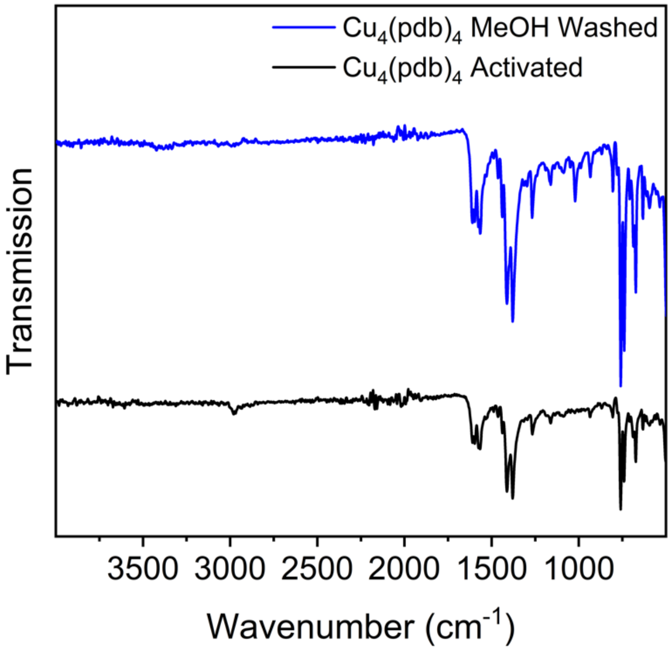

Figure S7. IR spectrum of $Cu_4(pdb)_4$ methanol solvated (blue) and activated (black).

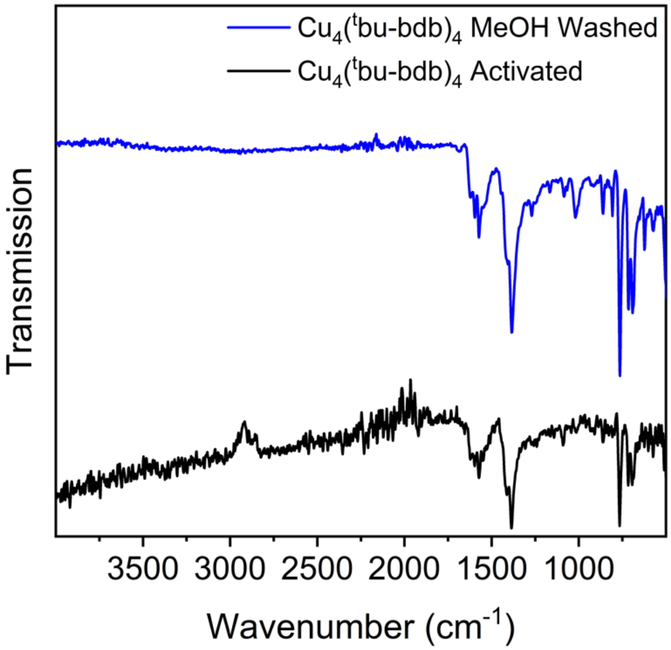

Figure S8. IR spectrum of $Cu_4(^tBu\text{-}bdb)_4$ methanol solvated (blue) and activated (black).

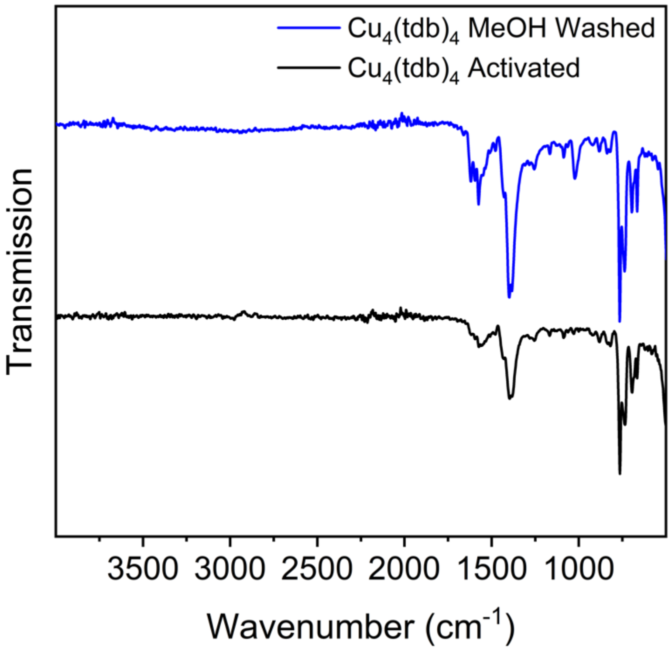

Figure S9. IR spectrum of $Cu_4(tdb)_4$ methanol solvated (blue) and activated (black).

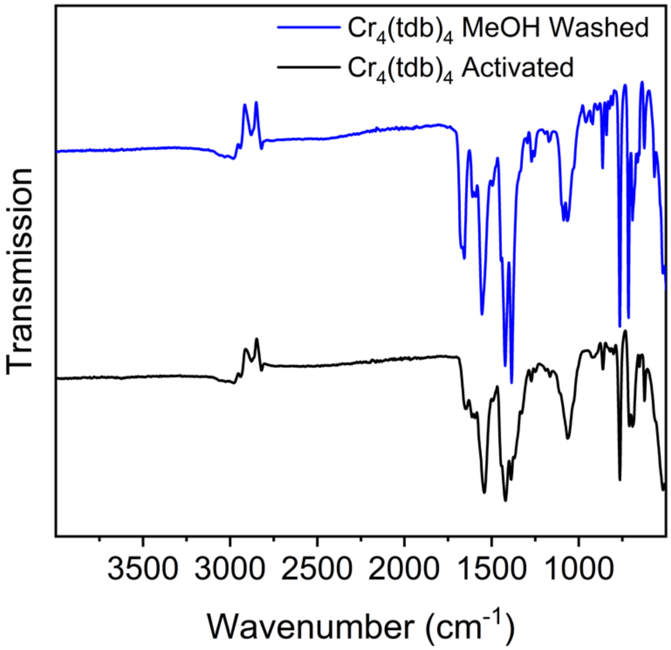

Figure S10. IR spectrum of $Cr_4(tdb)_4$ methanol solvated (blue) and activated (black).

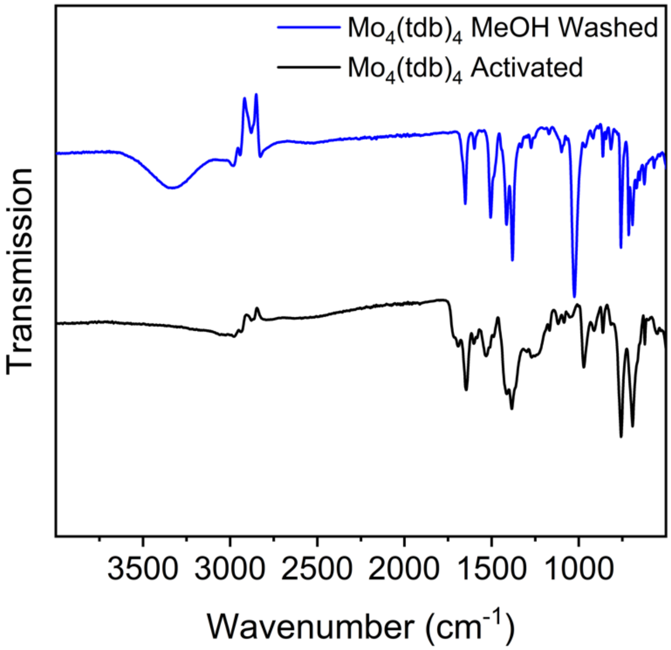

Figure S11. IR spectrum of Mo$_4$(tdb)$_4$ methanol solvated (blue) and activated (black).

X-Ray Crystallography:

X-ray structural analysis for $Cu_4(pdb)_4$, $Cr_4(tdb)_4$, [μ-Cl-$Mo_4(pdb)_4$] [μ-O-$Mo_4(pdb)_4$], and $Cu_4(tdb)_4$: Crystals were mounted using viscous oil onto a plastic mesh and cooled to the lowest achievable data collection temperature without thermally induced crystal damage (150K for $Cu_4(pdb)_4$ and $Cr_4(tdb)_4$, 175K for [μ-Cl-$Mo_4(pdb)_4$] [μ-O-$Mo_4(pdb)_4$], and, 200K for $Cu_4(tdb)_4$). Data were collected on a Bruker-AXS APEX II DUO CCD diffractometer with Cu-Kα radiation (λ = 1.54178 Å) focused with Goebel mirrors. Unit cell parameters were obtained from 48 data frames, 0.5° ω, from different sections of the Ewald sphere. The unit-cell dimensions, equivalent reflections and systematic absences in the diffraction data are uniquely consistent with *I*4, *I*-4, *I*4/m for $Cu_4(pdb)_4$, $Cr_4(tdb)_4$ and $Cu_4(tdb)_4$; and with *C*2, *C*2/*m* and *Cm* for [μ-Cl-$Mo_4(pdb)_4$] [μ-O-$Mo_4(pdb)_4$]. Refinement in the centrosymmetric space group options, *I*4/*m and C*2/*m*, yielded chemically reasonable and computationally stable results of refinement. The data were treated with multi-scan absorption corrections.[4] Structures were solved using intrinsic phasing methods[5] and refined with full-matrix, least-squares procedures on F^2.[6] The data-set of $Cu_4(pdb)_4$ was treated with a twin law (1 1 0) with a refined scale factor of 0.04.

Two similar molecules, each located at an intersection of a mirror plane and two-fold axis, were found in the asymmetric unit of [μ-Cl-$Mo_4(pdb)_4$] [μ-O-$Mo_4(pdb)_4$] with different central bridging atoms. The μ-O molecule is oriented with the tolyl ring plane perpendicular to the mirror while in the μ-Cl molecule the ligand-ligand angle is bisected by the mirror. The inner Mo…Mo distance in the μ-O molecule is 5.6630(14) Å while in the μ-Cl it is shorter despite the larger Cl atomic radius, 5.4770(14) Å, suggesting stronger metal-chloro interaction.

In $Cu_4(pdb)_4$, $Cr_4(tdb)_4$ and $Cu_4(tdb)_4$, the compound molecule is located at an intersection of a four-fold axis and a mirror plane with a coordinated DMF solvent found disordered along the four-fold axis in $Cu_4(tdb)_4$. Initial solutions of $Cu_4(pdb)_4$ displayed the bridging atom as an oblate ellipsoid perpendicular to the four-fold axis suggesting that the bridging atom is not located on the four-fold axis but was being disordered by it. The bridging atom was better modeled with its x and y axis constrained to be equal.

As in similar MOPs, the formula reported corresponds only to the atoms that could be reliably located or calculated, in the case of H-atoms. Residual electron density, solvent molecules and atoms that cannot be assigned a reasonable model, were treated as diffused electron density using Squeeze.[iv] These crystals were grown in mixtures of DMF and methanol solvents and we have no reliable non-crystallographic information to identify which solvent is present or, in the case of site disorder, the relative occupancy ratio of solvent molecules. The percentage volume treated as having diffused electron density contributions are 12.04, 11.81, and 30.36 % for $Cu_4(pdb)_4$, $Cr_4(tdb)_4$ and [μ-Cl-$Mo_4(pdb)_4$] [μ-O-$Mo_4(pdb)_4$], respectively.

Two symmetry equivalent voids of 210 $Å^3$ with 84 electrons, is suggestive of two DMF (2x40 or 80 electrons) per asymmetric unit or four DMF in the unit cell of $Cu_4(pdb)_4$ or two DMF per discrete molecule. In this case, each molecule would have the formula $C_{76}H_{44}Cu_4N_4O_{17}$ plus $2(C_3H_7NO)$ or $C_{82}H_{58}Cu_4N_6O_{19}$ with a formula weight of 1685.57 g/mol.

Similarly in $Cr_4(tdb)_4$, since a coordinated solvent O atom was modeled, two symmetry equivalent voids of 238 $Å^3$ with 61 electrons each could suggest two DMF [2x(40-8) or 64 electrons] per asymmetric unit, four in the unit cell or two per molecule. The would imply a formula of $C_{84}H_{56}Cr_4O_{19}$ plus $2(C_3H_7NO)$ less two O atoms or $C_{90}H_{70}Cr_4N_2O_{19}$ with a formula weight of 1691.53 g/mol.

In the unit cell of [μ-Cl-$Mo_4(pdb)_4$] [μ-O-$Mo_4(pdb)_4$], there are four voids, of which two are unique by symmetry, of 908 and 461 $Å^3$ containing 216 and 128 electrons, respectively. The smaller void could correspond to two coordinated DMF on the μ-O molecule each less the modeled CO [2x(40-14) electrons] plus four non-coordinated MeOH (72 electrons) which totals 124 electrons. The larger void could then be two coordinated DMF (80 electrons) on the μ-Cl molecule plus three non-coordinated DMF and one non-coordinated MeOH for a total of 218 electrons. This would suggest a [μ-Cl-$Mo_4(pdb)_4(DMF)_2$] [μ-O-$Mo_4(pdb)_4(DMF)_2$], solvated crystal phase with formula $(C_{84}H_{56}ClMo_4O_{18})(C_{84}H_{56}Mo_4O_{19})\bullet 3(C_3H_7NO)\bullet 5(CH_4O)$. While these extrapolations appear reasonable, alternative models that could satisfy the void electron counting could not be discounted. The true nature of the internal bridging oxygen moiety in these compounds also remains unclear.

Rigid bond restraints on thermal parameters were applied and additional three-dimensional restraints were applied for $Cu_4(pdb)_4$ and the DMF in $Cu_4(tdb)_4$. In order to conserve reasonable data-to-parameter ratios, only the metal atoms were refined with anisotropic displacement coefficients in $Cr_4(tdb)_4$ and [μ-Cl-$Mo_4(pdb)_4$] [μ-O-$Mo_4(pdb)_4$]. All other non-hydrogen atoms were refined with anisotropic displacement parameters. H-atoms were treated as idealized contributions with geometrically calculated positions and with U_{iso} equal to 1.2-1.5 U_{eq} or U_{iso} of the attached carbon atom. Atomic scattering factors are contained in the SHELXTL program library.[iii] The structures have been deposited at the Cambridge Structural Database under the following CCDC deposition numbers: 1998863-1998866.

Table S1. Crystal data summary and structure refinement details.

	$Cu_4(tdb)_4$	$Cu_4(pdb)_4$	$Cr_4(tdb)_4$	[μ-Cl-$Mo_4(pdb)_4$] [μ-O- $Mo_4(pdb)_4$]
Formula	$C_{90}H_{70}Cu_4N_2O_{19}$	$C_{76}H_{44}Cu_4N_4O_{17}$*	$C_{84}H_{56}Cr_4O_{19}$*	$C_{170}H_{112}ClMo_8O_{35}$*
Temperature (K)	200	150	150	175
Crystal system	tetragonal	tetragonal	tetragonal	monoclinic
Space group	*I*4/*m*	*I*4/*m*	*I*4/*m*	C2/m
Formula weight *M* (g/mol)	1737.64	1539.31	1577.28	3517.56
Unit cell dimensions				
a (Å)	12.8590(4)	12.121(4)	12.9890(11)	12.8297(7)
b (Å)	12.8590(4)	12.121(4)	12.9890(11)	26.2957(15)
c (Å)	23.9559(8)	23.730(6)	23.881(2)	27.2919
α (°)	90	90	90	90
β (°)	90	90	90	101.794(2)
γ (°)	90	90	90	90
V (Å^3)	3961.2(3)	3487(2)	4029.0(8)	9013.0(8)
Occupancy (*Z*)	2	2	2	2
Reflections collected / unique / R_{int}	10085 / 1074 / 0.0297	1519 / 1519 / 0.1184	10230 / 571 / 0.1002	19304 / 2825/ 0.0995
Final *R* indices [I>2σ] R_1 / wR_2	0.0739 / 0.2047	0.1521 / 0.4101	0.1447 / 0.4140	0.523 / 0.1285
R indices (all data) R_1 / wR_2	0.0863 / 0.2346	0.1854 / 0.4514	0.1742 / 0.4604	0.712 / 0.1398
CCDC	1998866	1998863	1998864	1998865

*Formulae and molecular weights correspond to identified atoms only. These structures have varying levels of modelling completion of the coordinated capping solvent which could be dimethylformamide and methanol. See additional details in SI.

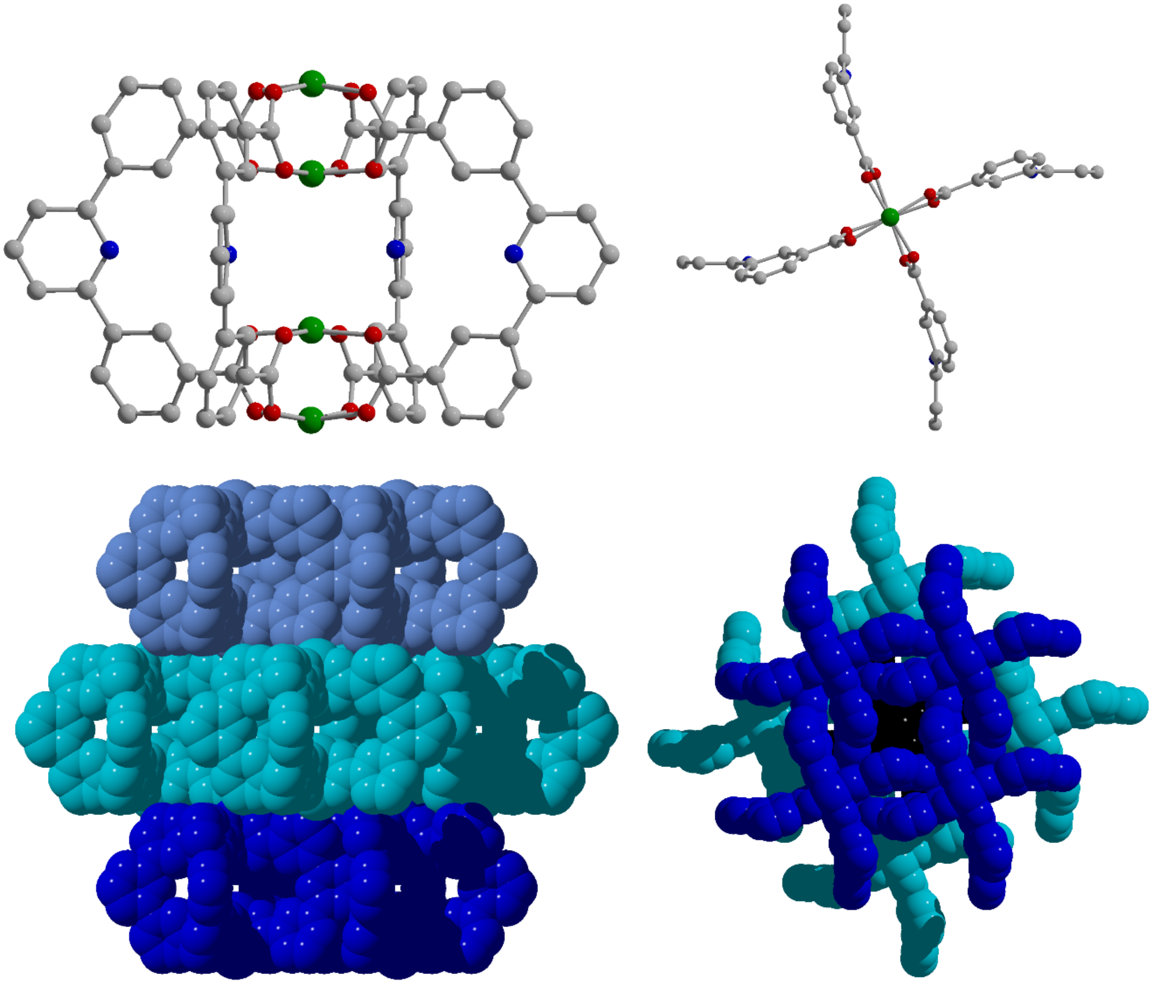

Figure S12. X-ray crystal structure of $Cu_4(pdb)_4$ viewed down the a-axis (Top Left) and the c-axis (Top Right). The space filled cage packing structure of $Cu_4(pdb)_4$ viewed down the a-axis (Bottom Left) and the c-axis (Bottom Right).

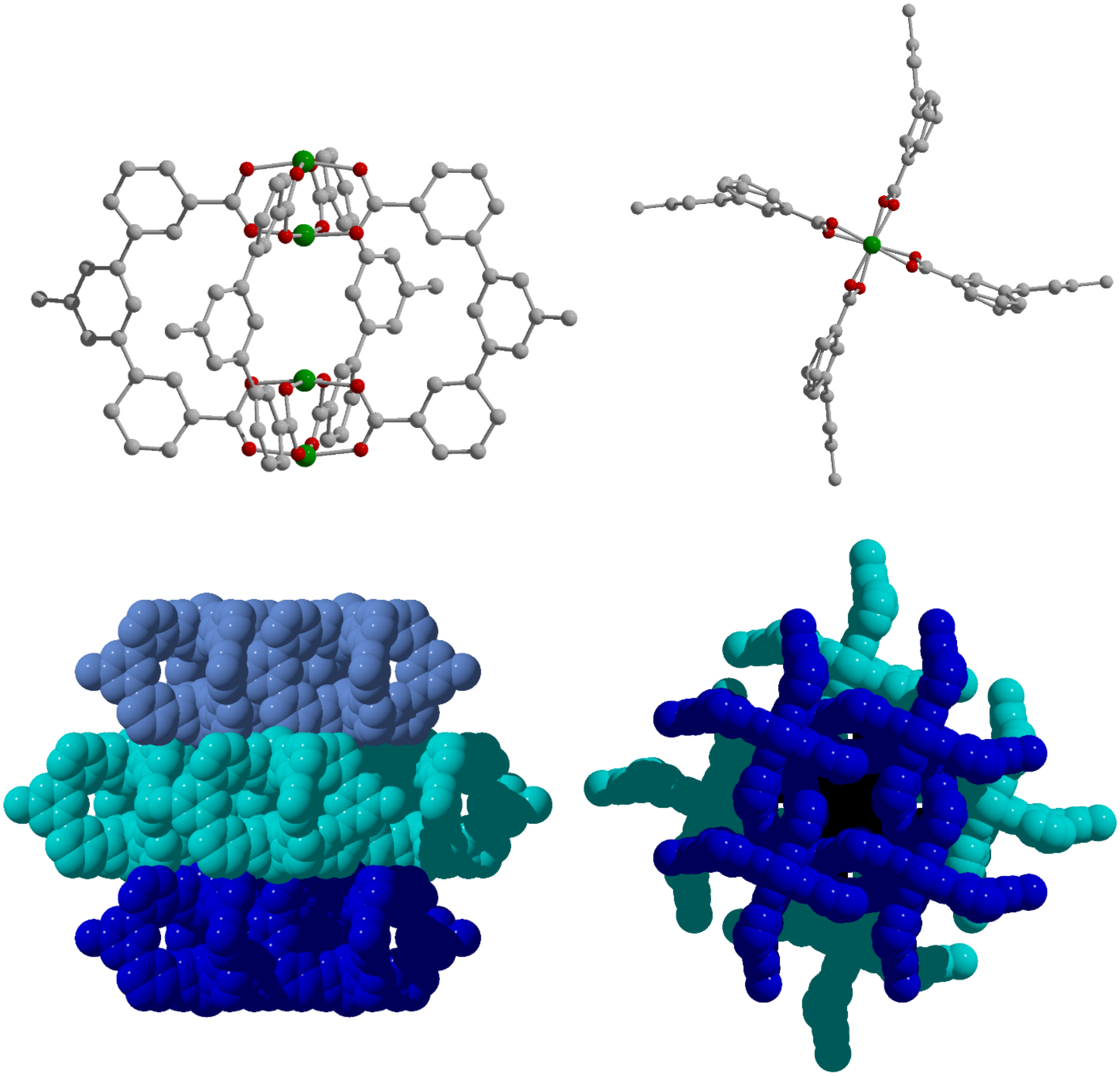

Figure S13. X-ray crystal structure of $Cu_4(tdb)_4$ viewed down the a-axis (Top Left) and the c-axis (Top Right). The space filled cage packing structure of $Cu_4(tdb)_4$ viewed down the a-axis (Bottom Left) and the c-axis (Bottom Right).

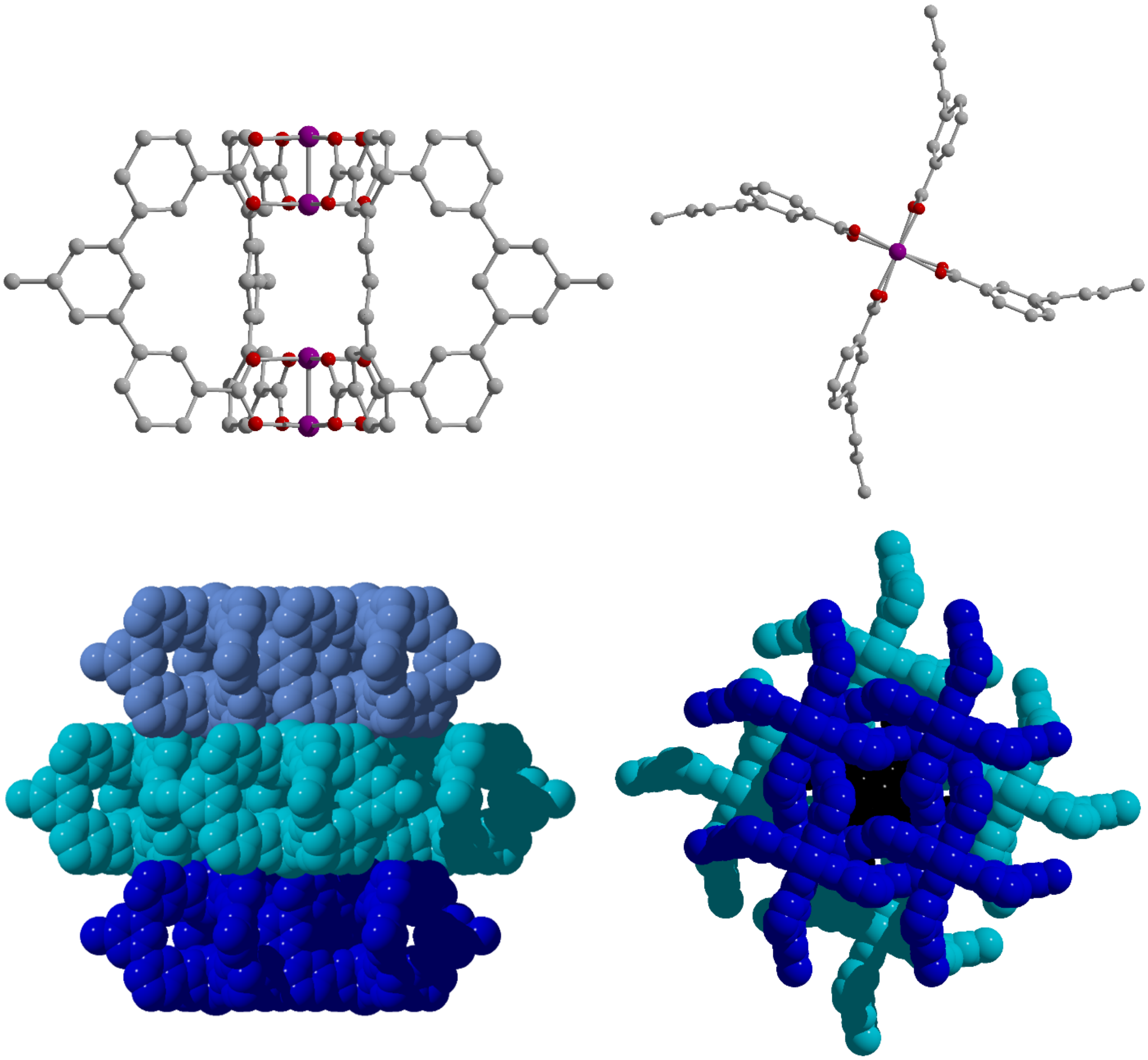

Figure S14. X-ray crystal structure of Cu$_4$(tdb)$_4$ viewed down the a-axis (Top Left) and the c-axis (Top Right). The space filled cage packing structure of Cu$_4$(tdb)$_4$ viewed down the a-axis (Bottom Left) and the c-axis (Bottom Right).

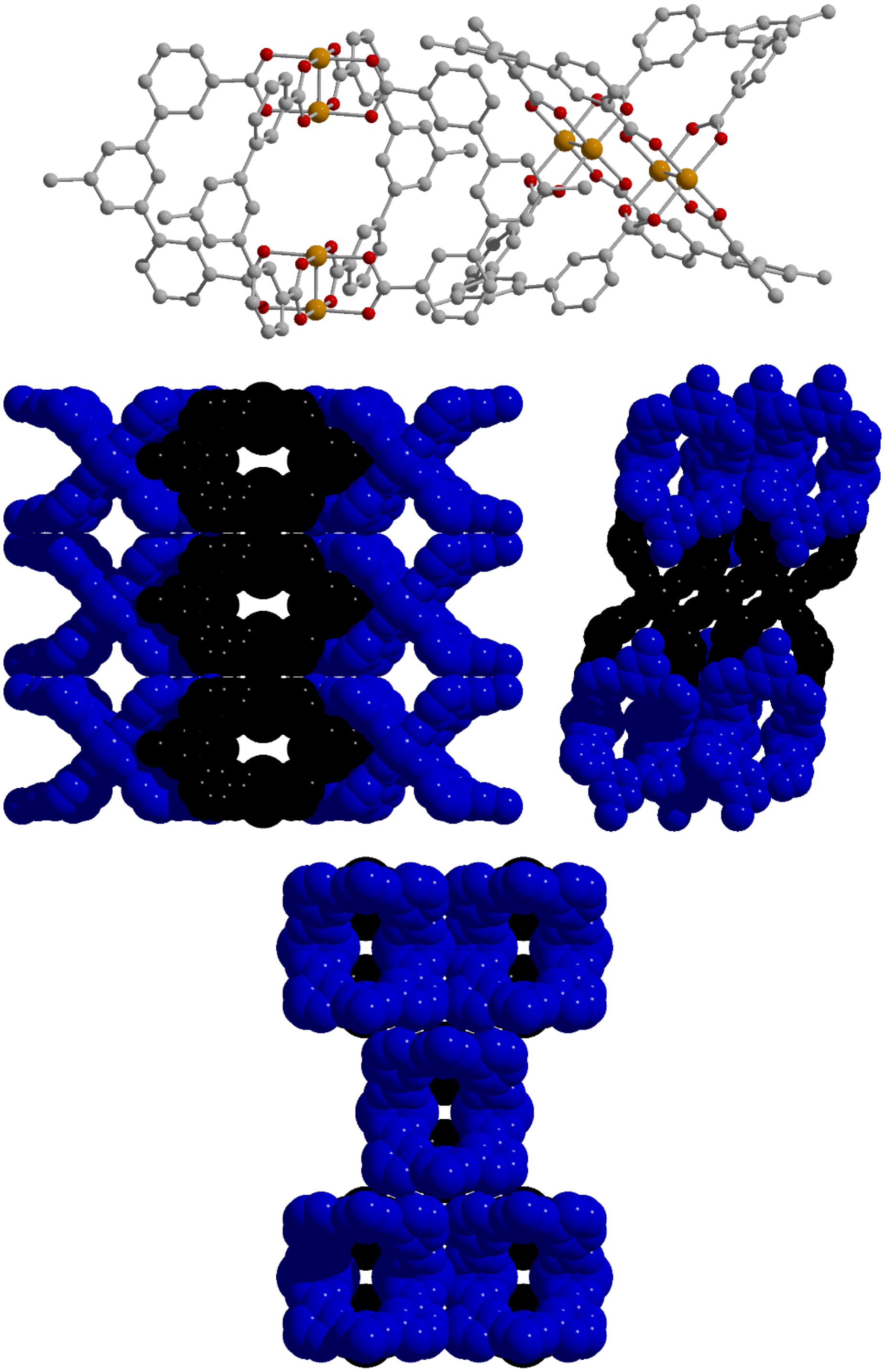

Figure S15. X-ray crystal structure of $Mo_4(tdb)_4$ (Top). The space filled cage packing structure of $Mo_4(tdb)_4$ viewed down the a-axis (Left), the b-axis (Right) and the c-axis (Bottom).

Powder X-Ray Diffraction:

X-ray powder diffraction patterns were taken at room temperature on a Rigaku MiniFlex powder diffractometer using filtered Cu Kα radiation (λ = 1.54178 Å).

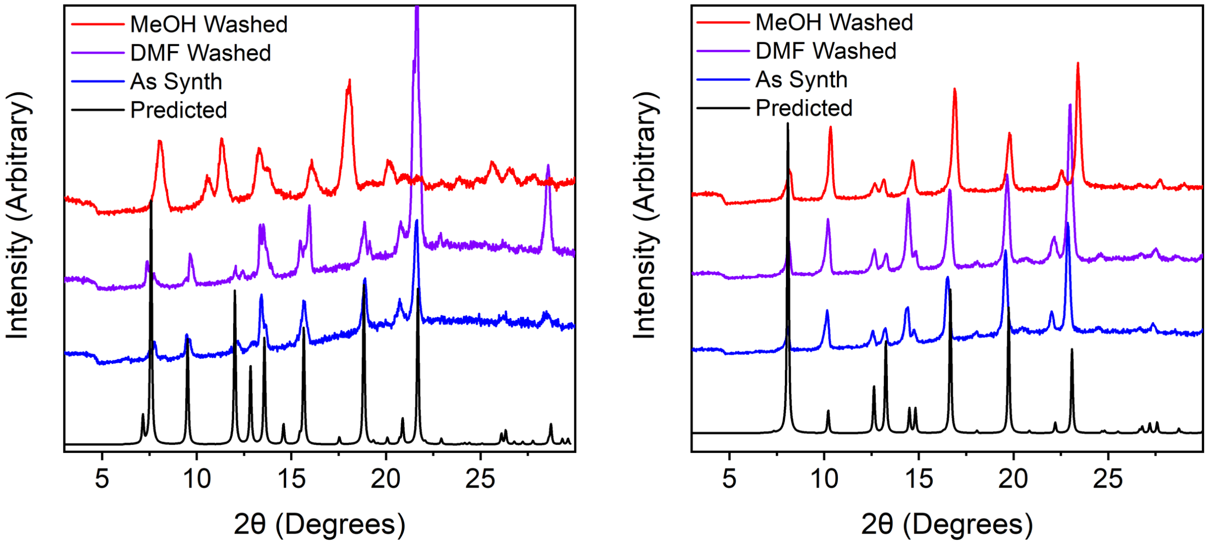

Figure S16. Powder X-Ray Diffraction patterns of $Cu_4(tdb)_4$ (Left) and $Cu_4(pdb)_4$ (Right). Black: simulated pattern, Blue: as synthesized material, Purple: DMF washed material, Red: Methanol washed material.

Synchrotron Powder diffraction:

Figures S17-S21 were collected at beamline 17-BM at the Advanced Photon Source Argonne National Laboratory at the wavelength of 0.45411 Å. The data was collected with the samples loaded in 2-mm capillaries with a sample to detector distance of 800 mm. Powder diffraction as a function of temperature was collected by a custom built setup to connect a turbo pump to the capillary. The data was converted from a diffraction image to a 2-dimentional powder pattern by GSAS-II.[6]

Pawley Refinement

Synchrotron x-ray powder diffraction patterns were analyzed using the program Topaz Academic.[7] The unit cell search feature was utilized to determine how the unit cell and space group changes upon methanol solvent exchange. Pawley refinements were performed on the best matching space groups to attempt to determine how the unit cell changes.[8] The unit cells that fit best had approximate axes of a = 21.91, b = 16.83, and c = 22.06 Å. A satisfactory space group could not be adequately determined between Aba2 (41) and Ccca (68). Further analysis could not be performed due to preferential orientation during data collection as seen in Figure S12 by the spots.

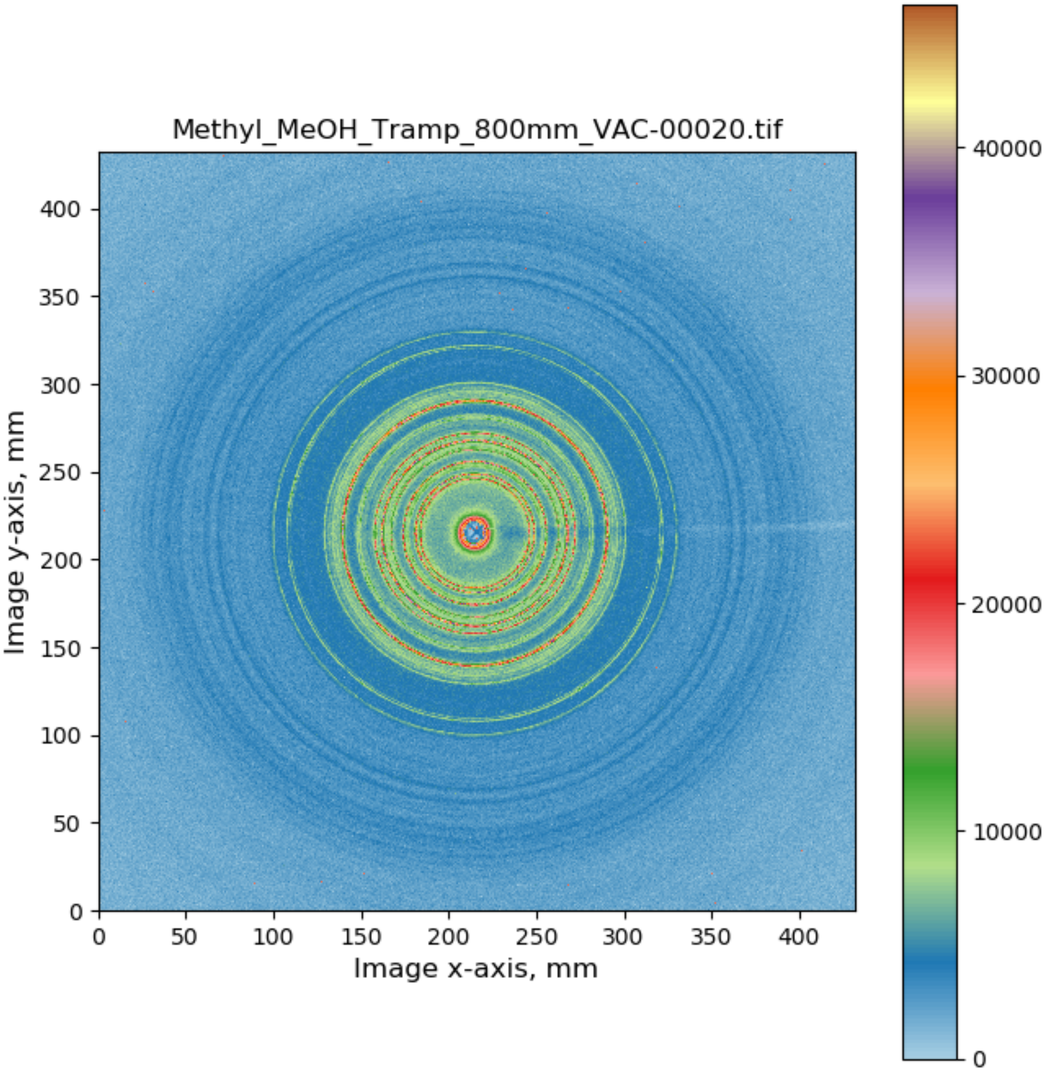

Figure S17. Powder diffraction pattern of $Cu_4(tdb)_4$ collected at 17-BM at the Advanced Photon Source Argonne National Laboratory.

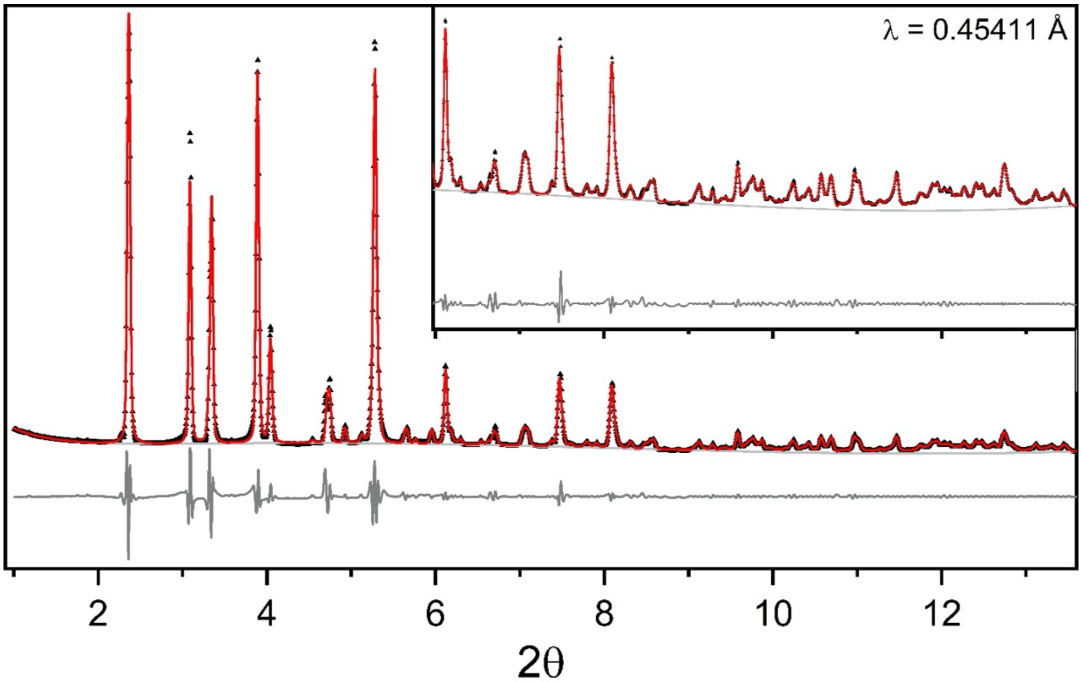

Figure S18. Pawley fit powder diffraction pattern of $Cu_4(tdb)_4$ heated to 498.7 K under vacuum.

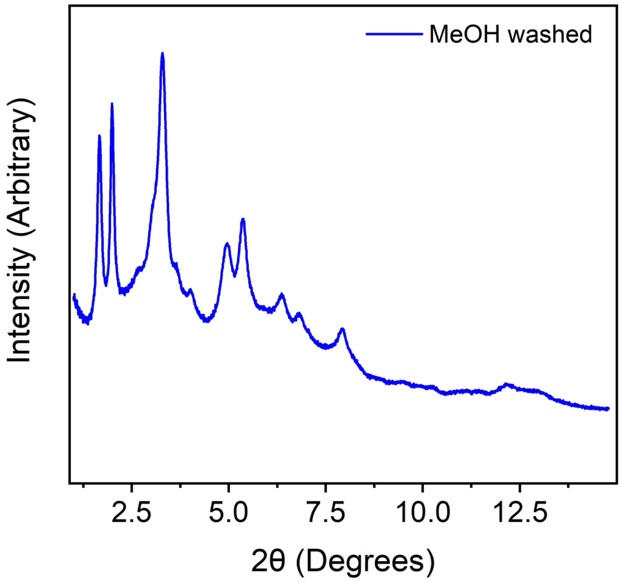

Figure S19. Powder X-Ray Diffraction pattern of methanol washed $Cu_4(^t\text{bu-bdb})_4$ collected at the Advanced Photon Source at Argonne National Lab.

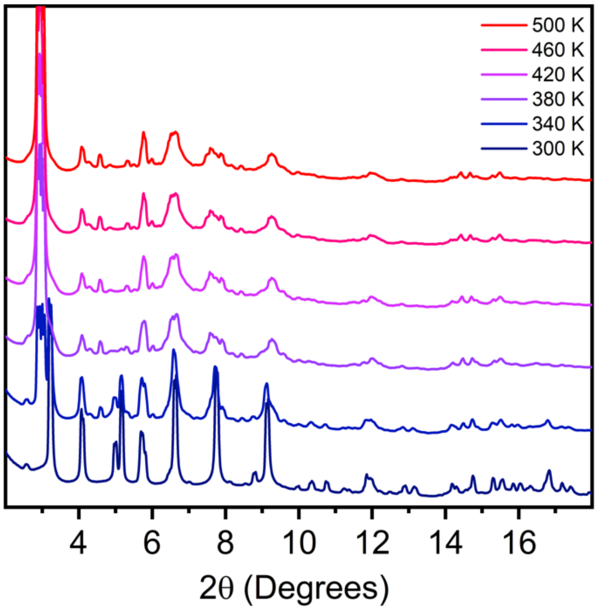

Figure S20. Powder X-Ray Diffraction patterns of methanol washed $Cu_4(pdb)_4$ collected under dynamic vacuum at the indicated temperatures at the Advanced Photon Source at Argonne National Lab.

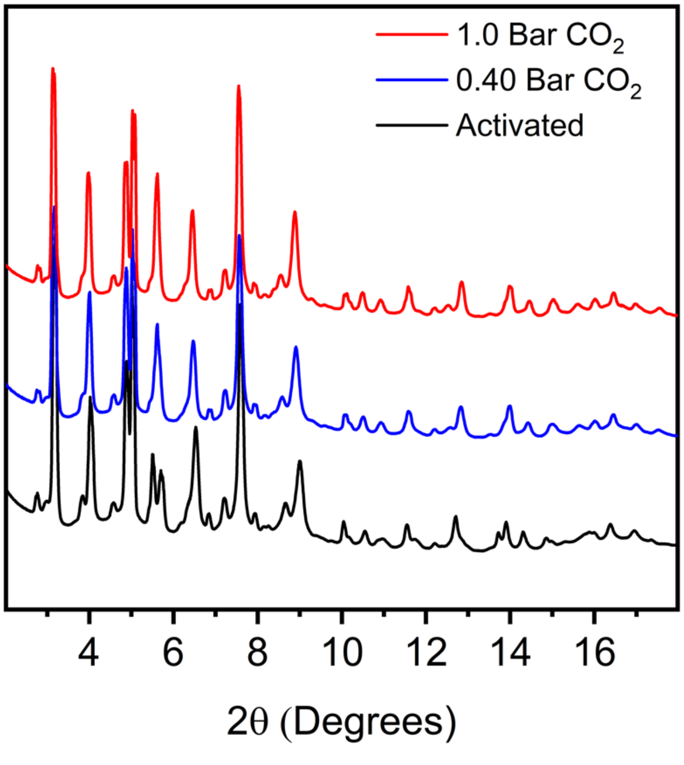

Figure S21. Powder X-Ray Diffraction patterns of activated $Cu_4(tdb)_4$ collected under dynamic vacuum (black) and at the indicated CO_2 dosing pressures at the Advanced Photon Source at Argonne National Lab.

Gas Adsorption:

All gas adsorption measurements were obtained with a Micromeritics 3Flexgas adsorption analyzer. The 3Flex tubes were evacuated on the Smartvac system after being heating in the oven to remove water. Once cooled and evacuated, the sealed tubes were weighed and then brought into the glove box. The samples were loaded into the tubes, sealed, removed from the glove box, and degassed overnight. Each sample was considered activated when the static outgas rate was less than 2 µbar/min. Once fully activated, the tube was weighed to determine an accurate mass of the sample. Surface areas and pore volumes were measured via CO_2 isotherm in a dry ice/isopropanol bath and calculated using the Micromeritics software. For these isotherms, typical equilibration times and dosing protocols were used. Specifically, 15 second equilibration times were programmed. In this approach, 10 increments (150 total seconds) elapsed after which equilibration was determined. Here a sample was considered equilibrated when the change in pressure after 15 seconds was less than 0.02 %. Adsorption points typically collected after 4-5 additional increments (14-15 total; ~220 seconds).

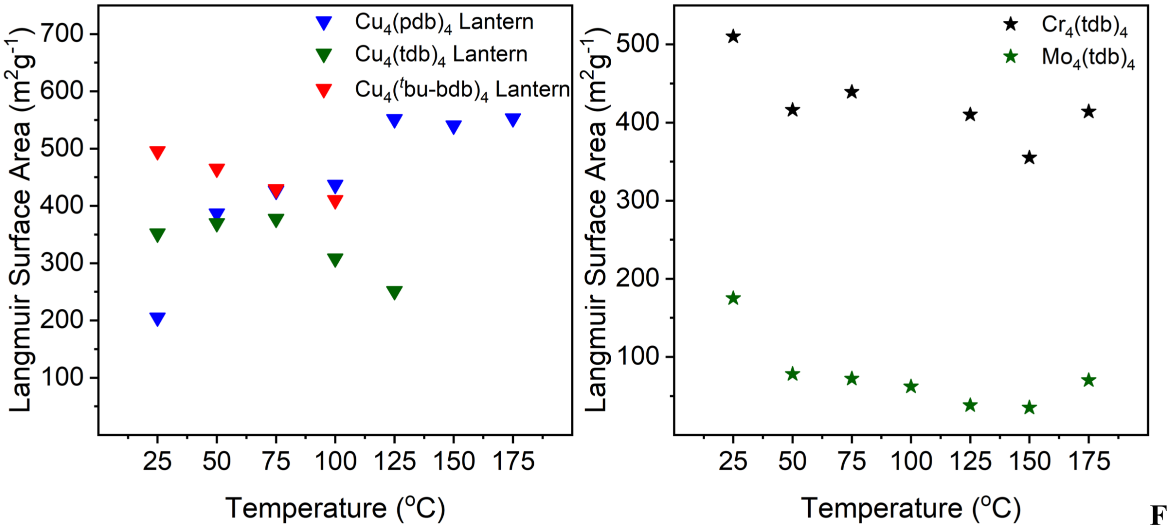

Figure S22. CO_2 Langmuir surface areas as a function of temperature for Cu_4L_4 lanterns (left) and N_2 Langmuir surface areas as a function of temperature for $Cr_4(tdb)_4$ and $Mo_4(tdb)_4$ (right).

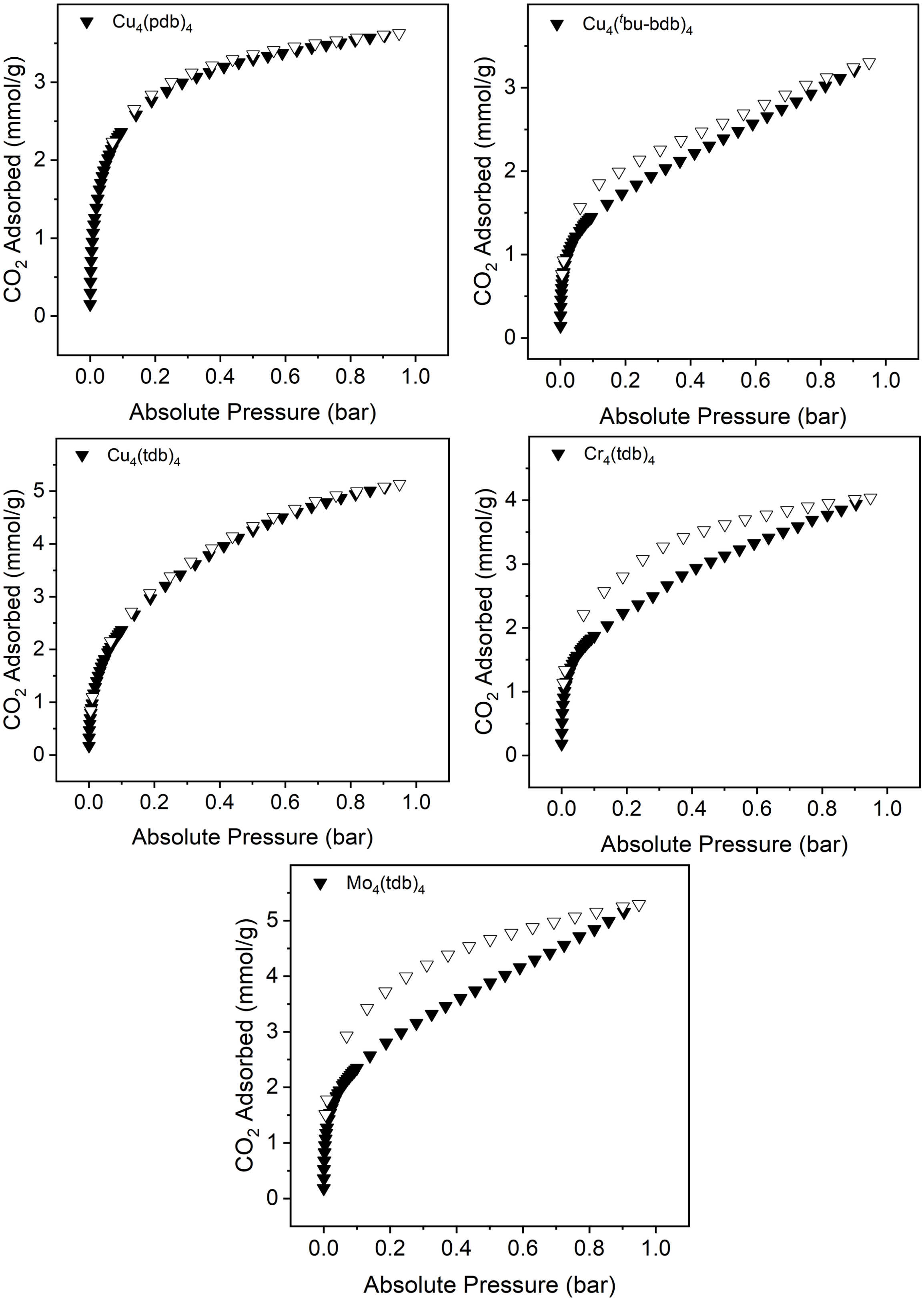

Figure S23. Full CO_2 BET isotherms of the M_4L_4 lanterns collected at 195 K. Closed symbol represents adsorption, open symbol denotes desorption.

Table S2. CO_2 Langmuir (BET) Surface Areas of M_4L_4 Lantern-Type Cages

Cage	CO_2 Surface Area (m^2/g)
$Cu_4(pdb)_4$	329 (195)
$Cu_4(^t$bu-bdb$)_4$	324 (113)
$Cu_4(tdb)_4$	527 (218)
$Cr_4(tdb)_4$	401 (145)
$Mo_4(tdb)_4$	516 (180.4)

References

1. O. Levy, B. Bogoslavsky, A. Bino, *Inorganica Chimica Acta.,* 2012, **391**, 179-181.
2. J.-R. Li, A. A. Yakovenko, W. Lu, D. J. Timmons, W. Zhuang, D. Yuan and H.-C. Zhou, *J. Am. Chem. Soc.*, 2005, **132**, 17599-17610.
3. R. Welti, Y. Abel, V. Gramlich and F. Diederich, *Helv. Chim. Acta*, 2003, **86**, 548-562.
4. Apex3; Bruker AXS Inc.: Madison, WI, 2015.
5. G. M. Sheldrick, *Acta. Cryst.,* 2015, **A71**, 3-8.
6. G. M. Sheldrick, *Acta. Cryst.*, 2015, **C71**, 3-8.
7. A. L. Spek, *Acta. Cryst*., 2015, **C71**, 9-18.